Stress rate sensitivity of Steel Fibre Reinforced Lightweight Concrete with Crumb Rubber

V. Bindiganavile[a], R. Mutsuddy and R. Cheng
University of Alberta, Edmonton, Canada

Abstract

Concrete with a compressive strength under 30 MPa is widely used to construct road-side barriers. However, its poor performance-to-weight ratio and the lack of material durability require continued search for alternative materials with improved shock absorption and acceptable resistance against severe environmental conditions. This paper reports a study on the impact resistance of lightweight steel fibre reinforced concrete. Along with an expanded shale lightweight coarse aggregate, crumb rubber was introduced as a replacement to fine aggregates at up to 75% by volume. All mixes had hooked end steel fibres at 1% volume fraction. The three mixes were designed varying in density between 1760 - 2130 kg/m^3. They were examined first under compression to establish reference constitutive response. Notched prismatic specimens were tested in flexure to evaluate the flexural strength and fracture toughness in Mode-I. Along with standard quasi-static flexural tests, a drop-weight impact tester with 1000 J capacity was used to generate stress rates in bending up to 10^8 kPa/s. The paper reports the stress rate sensitivity for both flexural strength and Mode I fracture toughness and highlights the effect of lightweight inclusions.

Keywords: Crumb Rubber; Drop-Weight Impact; Fracture Toughness; Stress Rate Sensitivity; Steel Fibres

---

a. Contact Author, (T) 001.780.492.9661; (F) 001.780.492.0249; (E) vivek.navile@gmail.com

1.0 Introduction

Accidents to motor vehicles on highways are a source of much loss to life and economic resources in Canadian society. Improving the crash cushioning capacity of road-side barriers can play a major role in minimizing these losses. Concrete road barriers have been in popular use over several decades. However, much remains to be improved including its impact resistance and energy absorption. At the same time, a key consideration in their manufacture and transport is their performance-to-weight ratio. In this study, a lightweight concrete mix was developed using an expanded shale aggregate and crumb rubber. The purpose was two-fold namely, to achieve efficient material composition for shock absorption and at the same time to promote the disposal and reuse of scrap tires across Canada.

According to ASTM C 825-06 [2006], the concrete usually used in road barriers should possess compressive strength less than 30 MPa. Lightweight aggregate concrete road barriers have been shown to be more durable against freeze-thaw, alkali-silica reaction and sulphate attack than conventional normal weight concrete [Burke, 2002; Holm and Ries, 2006]. Prior research has shown that recycled rubber from scrap tires can be used both as a fine aggregate and as a coarse aggregate to produce workable concrete [Eldin and Senouci, 1993; Khatib and Bayomy, 1999; Zheng et al. 2008]. Topcu [1995] found that the use of rubber as aggregate in concrete leads to higher amounts of energy absorption under both compressive and tensile loading. Topcu and Avcular [1997] showed that the impact resistance of concrete increases when rubber is used as the aggregate in concrete. However, the use of rubber is seen to cause a reduction in both compressive and tensile strength of concrete [Eldin and Senouci, 1993; Khatib and Bayomy, 1999]. Studies [Banthia et al. 1998; Bindiganavile and Banthia, 2005] show that using short fibres as discrete reinforcement largely improves the impact resistance and dynamic fracture toughness of conventional concrete. This study illustrates the response of steel fibre reinforced concrete containing manufactured and recycled lightweight aggregates under quasi-static and impact loading. The mixes were characterized first in quasi-static compression followed by a dynamic crack growth analysis in flexure. The dynamic responses were compared with existing CEB-FIP models [Comité Euro-International du Béton, 1990] to assess their stress rate sensitivity.

2.0 Experimental Program

The following parameters were examined to characterize their influence on the dynamic response of lightweight concrete containing crumb rubber:

- Crumb rubber as aggregate replacement: varied at 25% and 75% by volume of total fine aggregates;
- Rate of loading: quasi-static loading and impact from drop-height of 250 mm, 500 mm & 750 mm.

2.1 Materials

The cement used was a CSA A3001-08 [2008] Type GU ordinary Portland cement (OPC). A 10 mm downgraded expanded shale aggregate was used as the coarse aggregate. A locally available river sand and crumb rubber were variously used as the fine aggregate. The crumb rubber

aggregate were obtained in 3 size ranges (0.85 mm to 3.35 mm) and blended together in equal amount. From the distribution as shown in Figure 1, it is observed that the coarse aggregates are uniformly graded whereas sand and crumb rubber are fairly well graded. This blended aggregate was used at 25% and 75% volume replacement of total fine aggregates. The crumb rubber was manufactured from recycled motor vehicle tires and purchased from a local recycling company. Hooked-end steel fibres, 35 mm in length, aspect ratio of 65 and yield strength of 1100 MPa were employed at 1% volume fraction in all the mixes.

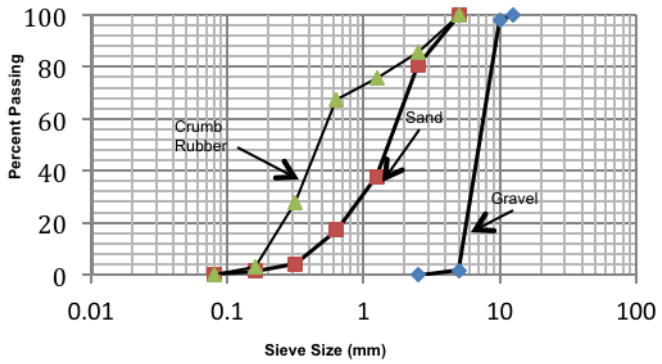

Figure 1: Grain Size Distribution of Coarse Aggregate, Fine Aggregate and Crumb Rubber

Table 1: Mix Proportions

Mix	w/b ratio	OPC	Expanded Shale	Sand	Crumb Rubber (% fine aggt. replaced)	Crumb Rubber (kg/m^3)	Steel Fibre (Volume Fraction) %	Hardened Density (kg/m^3)	Slump (mm)
		(kg/m^3)							
0% Rubber	0.4	550	986	640	0	0	1	2130	220
25% Rubber	0.4	550	986	480	25	51	1	2018	150
75% Rubber	0.4	550	986	160	75	153	1	1766	210

The mix proportions were based on a prior study to ensure a minimum strength of 15 MPa in compression [Wong & Ting, 2009]. This target minimum compressive strength is suitable for structural applications without exceeding the suggested upper limit for road barriers. In order to achieve a lower density than reported by Wong and Ting [2009], the present authors used a light weight expanded shale aggregate. The water-cementitious material ratio (w/cm) was 0.40 for all mixes. A high range water reducing admixture and an air entraining admixture were used to achieve adequate workability (100mm to 200mm slump) and air content (5% to 13%) respectively. The air content was deemed high enough to achieve adequate freeze-thaw resistance in the Alberta climate. The detail mix proportions for the resulting 3 mixes are given in Table 1.

2.2 Specimen Preparation

All specimens were prepared in accordance with ASTM C192 [2007] using a drum mixer of 75

litre capacity. From each mix, twelve 400 mm x 100 mm x 100 mm prisms were prepared to be tested in flexure. Three cylinders, 100 mm diameter and 200 mm height were also produced to be tested in compression. The specimens were demolded 24 hours after casting and then cured in a moist room under controlled humidity (> 99%) and temperature (22 ^{o}C) until testing. A 4 mm wide notch was sawn into each flexural specimen to a height of approximately 10 mm. This notch was intended to facilitate crack growth analysis under Mode-I fracture.

2.3 Test Setup

2.3.1 Compression Test

The compression tests were performed in accordance with ASTM C469 [2002] to evaluate the modulus of elasticity and establish the compressive stress-strain response. A displacement-controlled servo-hydraulic Materials Testing System with 2600 kN capacity was used to test the cylinders. Three longitudinal Linear Variable Displacement Transducers (LVDT) were placed at 120^{o} separation about the longitudinal axis together with two LVDTs in the transverse direction to measure axial and radial displacements respectively. The test arrangement is shown in Figure 2(a). The data was collected through a continuous-record data acquisition system at 10 Hz. The cross-arm displacement rate was set to 1.25 mm/min as recommended by ASTM C469, [2002]. The cylinders were sulphur capped to ensure plane surfaces conforming to ASTM C617 [2009].

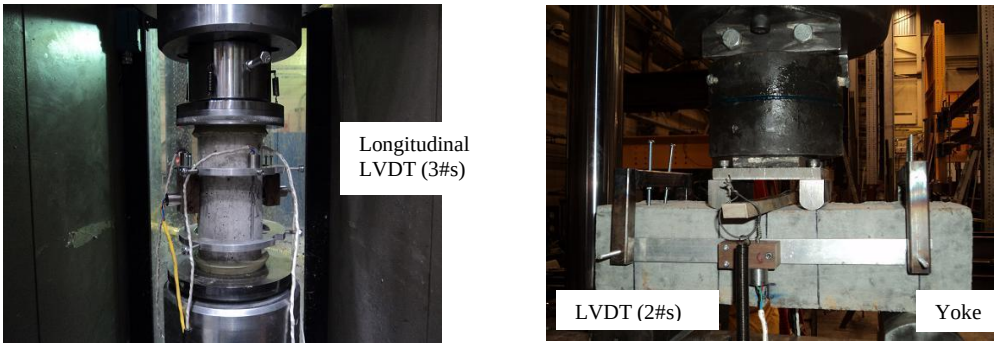

a) Compression Test Set-up b) Quasi-Static Flexural Test Set-up

Figure 2. Figure 2: Test Setup for Quasi-Static Testing

2.3.2 Flexural Test

2.3.2.1 Quasi-Static Test

From each mix, three prisms were tested in third-point bending according to ASTM C1609 [2010]. A Material Testing System of 1000 kN capacity was used for this purpose. The load was applied by setting the cross-arm displacement rate to 0.15 mm/min which conformed to ASTM C1609 [2010]. As shown in Figure 2(b), a yoke was installed around the specimens to attach two LVDTs, one on either side. This yoke ensured that the displacement measured was that of the neutral axis

and eliminated any errors due to support settlement. The load and displacement readings were sampled at 10 Hz.

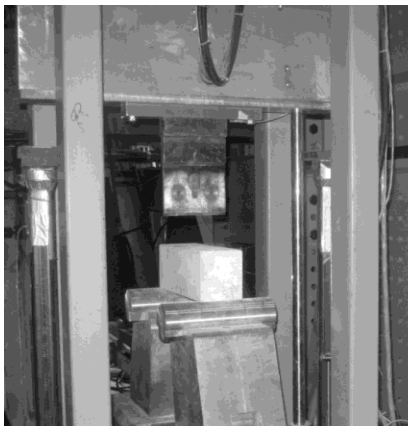

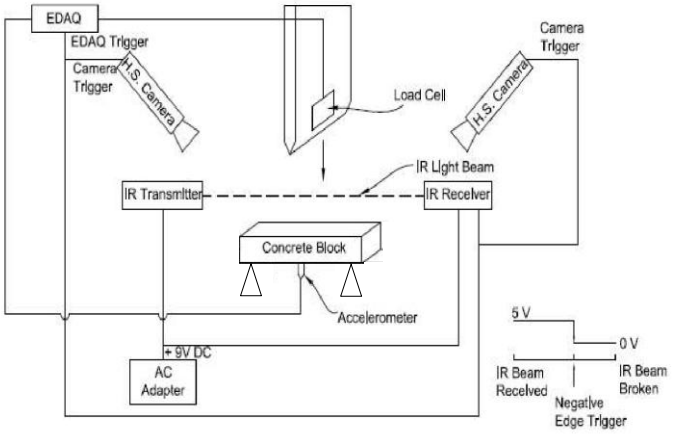

a) Drop Weight Impact Machine b) Schematic of the Trigger Mechanism [Islam, 2010]

Figure 3: Instrumented Drop-Weight Impact Tester

3.4.2.2 Impact tests

Dynamic flexural tests were conducted in an instrumented drop weight impact machine shown in Figure 3. A 62 kg hammer was released from three different drop heights of 250mm, 500mm and 750mm to achieve increasing stress rates in the samples. Three prisms were tested from each drop height. A piezoelectric accelerometer was attached underneath the test specimen next to the notch at mid span in order to capture the acceleration time history. The total impacting load (including the inertial load) was recorded by using a bridge loading device (tup) attached to the striking knife edge. Two high speed cameras were also installed to obtain a stereoscopic record of the impact test. The accelerometer and load cell recorded data at 100,000 Hz while the two cameras captured images at a frequency of 10,000 frames per second. A trigger mechanism was installed so that all four sets of data (i.e. from the accelerometer, the load cell and the two high speed cameras) were synchronized to the same time-stamp. Later, the images were analyzed using image processing software to measure the crack mouth opening displacement (CMOD) and vertical displacement for each individual specimen. From the image analysis, the values of mid span deflection and CMOD were plotted and a best fit straight line passing through the origin is drawn to get a linear relationship between them. The relationship between CMOD and displacement was used to determine the stress intensity factor of the specimen based on the formulation by Guinea et. al. [1998] from which the crack growth resistance curve and fracture toughness were calculated. The inertial component of the applied load was accounted for as described by Banthia et. al. [1989]. Assuming a linear acceleration distribution along the span and using the virtual work principle, the generalized inertial load can be calculated using Equation 1.

$$P_1(t) = A\,\ddot{u}(t)\rho\left(\frac{S}{2} + \frac{l^2}{3S}\right) \quad [1]$$

where, S = span, l = overhang, A = cross-sectional areal; ρ = mass density and, (t) = acceleration at mid span at any time t. The effective bending load was computed by subtracting the inertial load from the recorded total load captured by the bridge loading tup. Further analyses were carried out to compute the displacement time history, $\Delta_0(t)$, at the location of the accelerometer from the acceleration history, $\ddot{u}(t)$, as described by Equation 2.

$$\Delta_0(t) = \iint \ddot{u}(t)\,.\,dt\,.\,dt \quad [2]$$

3.0 Results and Discussion

3.1 Compressive Response

The stress-strain response of different mixes under compression is shown in Figure 4. The compressive strength and modulus of elasticity are listed in Table 2. The modulus of elasticity was calculated as per ASTM C469. In CSA A23.3-04 [2004], the modulus of elasticity of plain concrete is calculated from the compressive strength using Equation 3,

$$E_c = (3300\sqrt{f'_c}+6900)(\gamma_c/2300)^{1.5} \quad [3]$$

where, γ_c = Unit weight of concrete and f'_c = Compressive strength in MPa. It is noted that an increase in rubber content from 25% to 75% by volume replacement of sand causes the compressive strength to drop to one-third of its value. In this same regime, the modulus of elasticity decreased by 33%. The suggested value of modulus of elasticity derived from Equation 3 is compared with the experimental values in Table 2. For lower rubber content the variation in theoretical and experimental modulus of elasticity was lower than that with higher rubber content.

3.2 Flexural Response

3.2.1 Quasi-Static Response

The load-deflection response under third-point bending is shown in Figures 4b-d. Since a notch was introduced, the modulus of rupture, f'_R was calculated using the effective cross sectional dimensions after accounting for the notch. The post peak energy dissipation was evaluated as per ASTM 1609 [2010] for fibre reinforced concrete. This method introduces an equivalent flexural strength ratio ($R^D_{T,150}$) as calculated by using Equation 4.

$$R^D_{T,150} = 150*T^D_{150}/(f_1*b*d^2) \quad [4]$$

where, T^D_{150}= toughness up to a net deflection of L/150,
f_1 = first Peak Strength,

b = average width of the specimen at fracture,
d = average depth of the specimen at fracture.

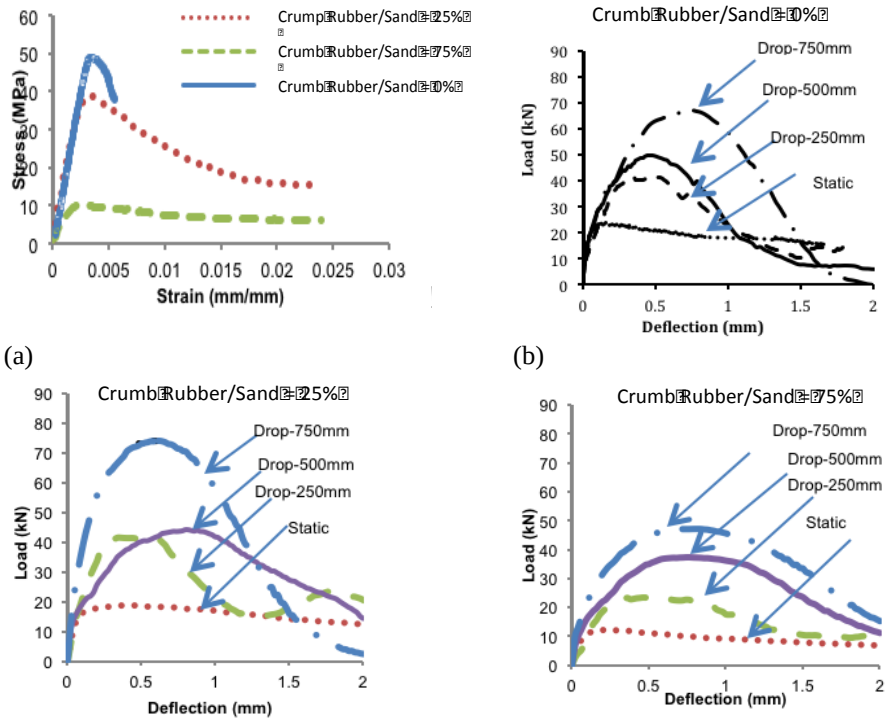

Figure 4: a) Compressive Response; b) Flexural Response for Mix Containing no Crumb Rubber; c) Flexural Response for Mix Containing 25% Crumb Rubber Substitution; d) Flexural Response for Mix Containing 75% Crumb Rubber Substitution

Table 2: Summary of quasi-static compression and flexure response

Mix Description	f'_c (MPa)	E_c (MPa)	E_c (Test)/ E_c (CSA)	f'_R (Quasi-static) (MPa)	$R^D_{T,150}$ (Quasi-static), %
(OPC, 0% Rubber)	45	19440	0.75	9.7	77
(OPC, 25% Rubber)	39	15300	0.88	7.0	84
(OPC, 75% Rubber)	12	7800	0.64	4.6	73

A summary of the quasi-static flexural properties is provided in Table 2. There was a significant drop in f'_R value as well as in case of the equivalent flexural strength with an increase in the rubber content. Armelin and Banthia [1997] proposed that the mid span deflection of the beam, Δ, and the crack mouth opening displacement, CMOD, are related according to the following equation,

$\Delta = 0.75 * CMOD$ [5]

Using this relation, the stress intensity factor was calculated from the load-deflection response as propose by prior researchers [Guinea et al., 1998; Broek D, 1986]. The resulting crack growth resistance curves are shown in Figure 5 and the fracture toughness K_{IC} was determined for all mixes, as listed in Table 3.

Table 3: Dynamic Response under Flexural Impact

Mix Description	f'_R (250mm) (MPa)	$R^D_{T,150}$ (250mm), %	f'_R (500mm) (MPa)	$R^D_{T,150}$ (500mm), %	f'_R (750mm) (MPa)	$R^D_{T,150}$ (750mm), %
(0% Rubber)	27.5	31.9	32.5	30.5	35.1	36.8
(25% Rubber)	23.7	40.0	28.6	41.0	42.1	37.0
(75% Rubber)	13.1	45	21.0	48.0	26.5	50.0

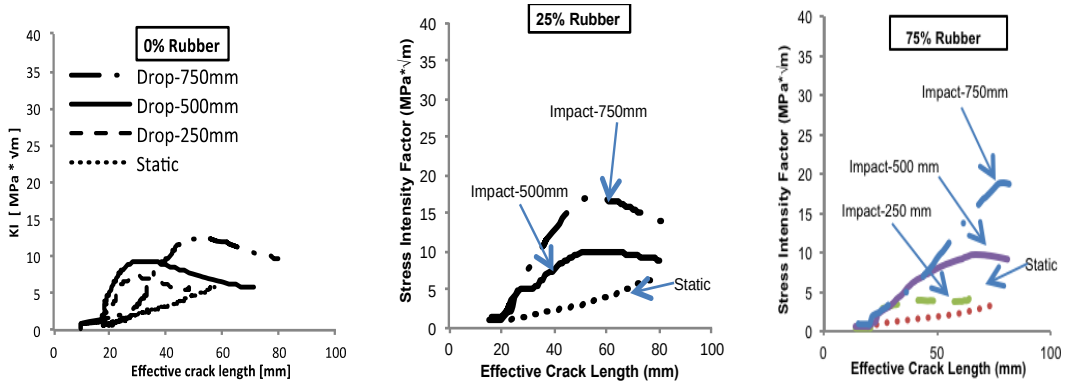

Figure 5. Crack Growth Resistance (R-Curves), Showing Stress Intensity Factor

3.2.2 Dynamic Response

The results from the impact tests were analyzed to derive the load-deflection responses, which are shown in Figures 4b-d. From these plots, the equivalent flexural strength ratio and modulus of rupture were calculated and are summarized in Table 3. Using images from the stereoscopic high speed imaging system, the CMOD and corresponding mid span deflection were recorded. A best fit straight line similar to Equation [6] was drawn for those recorded values.

$\Delta = m * CMOD$ [6]

where, Δ = mid span deflection;
m = slope of the straight line;
CMOD = crack mouth opening displacement.
The slope, m, as obtained from the present study was almost similar (±10%) to that derived by Armelin and Banthia [1997]. Thus, the crack growth resistance curves were derived as shown in Figure 5, in a manner similar to the quasi-static analysis (Guinea et al., 1998; Broek D, 1986). The dynamic fracture toughness is shown in Table 3.

3.2.3 Stress Rate Sensitivity

The stress rate sensitivity of flexural strength is shown in Figure 6, where the experimental values are compared with the stress rate sensitivity model proposed by CEB-FIP. The results show that in general the CEB-FIP model uniformly underestimates the stress-rate sensitivity of mixes containing crumb rubber. Again, to describe the stress rate sensitivity, Nadeau et al. [1982] has also proposed the following equation,

$$\ln \sigma_f = \frac{1}{N+1} \ln B \dot{\sigma} + \frac{1}{N+1} \ln(\sigma_i^{N+2} - \sigma_f^{N+2}) \quad [7]$$

where,

σ_f = stress at final condition, σ_i = stress at initial condition

B, N = constant, $\dot{\sigma}$ = stress rate

The stress rate is dependent on the relative density of materials. As the specimens considered here has different density, a plot of log strength versus log stress rate yields a line with a slope of 1/(N+1). The parameter N is dependent on material strength and stress-rate and a lower N-value denotes higher stress rate sensitivity. It was observed that mixes with higher rubber content were more sensitive to stress rate. Although there is no model available to predict the stress rate sensitivity for fracture toughness, it was evident that the mixes with higher rubber content were more sensitive to stress rate. Hence, adding crumb rubber to concrete is conducive to its use as a sacrificial material to absorb shock during the impact loading. Again, due to lower density, these mixes will provide better performance to weight ratio for this particular type of application.

4.0 Concluding Remarks

This study explored the dynamic performance of lightweight concrete that contains crumb rubber as volume replacement of sand. There was a significant reduction in the compressive strength and modulus of elasticity. While there was a drop in the modulus of rupture with an increase in rubber content, the fracture toughness was similar regardless of the rubber content. As expected with lighter composites, the modulus of rupture and fracture toughness were more sensitive to stress rate for higher rubber content. Clearly, due to its lighter density, mixes with crumb rubber are attractive as shock absorbing composites. However, as this study did not consider aspects of durability, it is recommended that the lighter mixes be examined for air-void network and bond with reinforcement.

5.0 Acknowledgement

The authors thank the Centre for Transportation Engineering and Planning (CTEP-Alberta) for the financial support to this study.

6.0 References

1. Armelin HS, Banthia. 1997. *Predicting the Flexural Postcracking Performance of Steel Fibre Reinforced Concrete from the Pullout of Single Fibers*. ACI Mater J 94(1):18-31

2. ASTM C 825-06. 2006. *Standard Specification for Precast Concrete Barriers*. ASTM International, W. Conshohocken, PA.
3. ASTM C 192-07. 2007. *Standard Practice for Making and Curing Concrete Test Specimen in the Laboratory*. ASTM International, W. Conshohocken, PA.
4. ASTM C1609-10. 2010. *Standard Test Method for Flexural Performance of Fibre-Reinforced Concrete (using beam with third point loading)*. ASTM International, W. Conshohocken, PA.
5. ASTM C469-02e1. 2002. *Standard Test Method for Static Modulus of Elasticity and Poisson's Ratio of Concrete in Compression*. ASTM International, West Conshohocken, PA.
6. ASTM C617-09a. 2009. *Standard Practice for Capping Cylindrical Concrete Specimens.* ASTM International, West Conshohocken, PA.
7. Banthia, N., Mindess, S., Bentur, A. and Pigeon, M. 1989. *Impact Testing of Concrete using a Drop-Weight Impact Machine*. *Experimental Mechanics*: 63-69.
8. Banthia, N., Yan, C. and Sakai, K. 1998. *Impact Resistance of Fiber Reinforced Concrete at Subnormal Temperature*. Cement and Concrete Composites, 20(5): 392-404
9. Bindiganavile, V. and Banthia, N. 2005. *Generating Dynamic Crack Growth Resistance Curves for Fiber-reinforced Concrete. Society for Experimental Mechanics.* 45(2):112-122.
10. Broek D.,(1986). *Elementary Engineering Fracture Mechanics*. Kluwer Academic Publishers, Dordrecht, The Netherlands.
11. Burke, D.F. and Drake, J. E. 2002. *Durable Lightweight Concrete for the Modular Hybrid Pier (State-Of-The-Art)*. Technical Report TR-2205-SHR, Naval Facilities Engineering Service Center, Port Hueneme, California.
12. CEB-FIP 1990: CEB-FIP Model Code 90, *Comite Euro-International du Beton –Federation Internationale de la Precontrainte*, Redwood Books, Trowbridge, Wiltshire, UK, 1990.
13. CSA A23.3-04. 2004. *Design of Concrete Structures*. Canadian Standards Association, Mississauga, ON
14. CSA A3001-08. 2008. *Cementitious Materials Compendium*. Canadian Standards Association, Mississauga, ON
15. Eldin, N. N., and Senouci, A. B. 1993. *Rubber-tire Particles as Concrete Aggregate*. J. Mater. Civ. Eng., 5(4): 478–496
16. Guinea GV, Pastor JY, Planas J,Elices M .1998 *Stress Intensity Factor, Compliance and CMOD for a General Three-point-bend Beam*. Int J Fract 89:103-116
17. Holm, T.A. and Ries, J. 2006. *Lightweight Concrete and Aggregates*. Significance of Tests and Properties of Concrete and Concrete Making Materials, STP 169D, ASTM International, West Conshohocken, PA.
18. Islam, M. T., 2010. *Static and dynamic response of sandstone masonry units bound with fibre reinforced mortars*. M.Sc. Thesis, University of Alberta.
19. Khatib, Z. K., and Bayomy, F. M. 1999. *Rubberized Portland Cement Concrete*. Journal of Materials in Civil Engineering, 11(3): 206-213
20. Nadeau, J.S., Bennett, R. and Fuller Jr., E.R., (1982). *'An Explanation for the Rate-of-Loading and the Duration-of-Load Effects in Wood in terms of Fracture Mechanics'*, J. of Mat. Sc., (17): 2831-2840.
21. Topcu, I. B. 1995. *The properties of rubberized concretes*. Cement and Concrete Research 25(2):304–310
22. Topcu, I. B. and Avcular, N. 1997. Collision behaviours of rubberized concrete. Cement and Concrete Research 27(12):1893–1898
23. Wong, Sook-Fun and Ting, Seng-Kiong. (2009). *Use of Recycled Rubber Tires in Normal and High-Strength Concretes*. 106(4): 325-332.
24. Zheng, L., Sharon Huo X., and Yuan, Y. (2008). *Strength, Modulus of Elasticity and Brittleness Index of Rubberized Concrete*. *J. of Mat. in Civil Engineering.*, 20(11): 692-699.